Applications of Mathematics

Roman Kohut

Parallel solution of elasticity problems using overlapping aggregations

Applications of Mathematics, Vol. 63 (2018), No. 6, 603–628

Persistent URL: http://dml.cz/dmlcz/147560

Terms of use:

© Institute of Mathematics AS CR, 2018

Institute of Mathematics of the Czech Academy of Sciences provides access to digitized documents strictly for personal use. Each copy of any part of this document must contain these *Terms of use*.

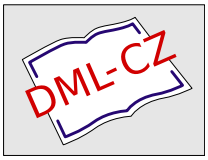

This document has been digitized, optimized for electronic delivery and stamped with digital signature within the project *DML-CZ: The Czech Digital Mathematics Library* http://dml.cz

63 (2018) APPLICATIONS OF MATHEMATICS No. 6, 603–628

PARALLEL SOLUTION OF ELASTICITY PROBLEMS USING OVERLAPPING AGGREGATIONS

Roman Kohut, Ostrava

Received May 29, 2017. Published online June 12, 2018.

Abstract. The finite element (FE) solution of geotechnical elasticity problems leads to the solution of a large system of linear equations. For solving the system, we use the preconditioned conjugate gradient (PCG) method with two-level additive Schwarz preconditioner. The preconditioning is realised in parallel. A coarse space is usually constructed using an aggregation technique. If the finite element spaces for coarse and fine problems on structural grids are fully compatible, relations between elements of matrices of the coarse and fine problems can be derived. By generalization of these formulae, we obtain an overlapping aggregation technique for the construction of a coarse space with smoothed basis functions. The numerical tests are presented at the end of the paper.

Keywords: conjugate gradients; aggregation; Schwarz method; finite element method; geotechnical application; elasticity

MSC 2010: 65F08, 74S05

1. Introduction

A practical geotechnical elasticity problem is usually characterized by large dimensions and strong heterogeneity. The finite element discretization of this problem on the domain Ω leads to a large sparse symmetric positive definite (SPD) linear system, $Au = f$. To solve it, we need an efficient iterative solver. For the SPD problems, it is very efficient to use the preconditioned conjugate gradient method. When using parallel computers, it is suitable to use a domain decomposition (DD) method as a preconditioner (see [4]). The domain decomposition refers to the process of subdividing the solution of a large linear system into smaller problems on subdomains, the solution of which can be used to construct the preconditioner.

Supported by the project IT4Innovations Excellence in Science (No. LQ1602) of the Ministry of Education, Youth and Sports of the Czech Republic.

DOI: 10.21136/AM.2018.0142-17

Using the FE discretization, the domain Ω is assumed to be divided into a set of elements $\mathcal{T}_h(\Omega)$ which defines the finite element space $V = V_h$,

$$V_h(\Omega) = \{v \in C(\bar{\Omega}) \cap \mathcal{V}\colon\ v|_{e_h} \in P_1(e_h)\ \forall\, e_h \in \mathcal{T}_h(\Omega)\}. \tag{1.1}$$

If $\mathcal{T}_h(\Omega)$ is composed of tetrahedra, $P_1(e_h)$ denotes the set of linear polynomials on the tetrahedral element e_h. If $\mathcal{T}_h(\Omega)$ is composed of hexahedra, $P_1(e_h)$ denotes the set of trilinear polynomials on the hexahedral element e_h. Furthermore, $\mathcal{V}$ is the space of functions satisfying the homogeneous Dirichlet boundary conditions prescribed on a part of the boundary $\partial\Omega$.

We use structural grids in our case. The position of each node is given by a triplet of indices and the corresponding nodal coordinates $(x(i,j,k), y(i,j,k), z(i,j,k))$. The general structural grid with $n_x \times n_y \times n_z$ nodes corresponds to the rectangular uniform "index" grid, where the node in position (i,j,k) has coordinates (i,j,k). In this case, the domain Ω is divided into $n_z - 1$ layers of hexahedra with $(n_x - 1) \times (n_y - 1)$ hexahedra in each layer. If we use tetrahedral elements, each hexahedron is further divided into six tetrahedral elements. This decomposition determines the corresponding structure of the set $\mathcal{T}_h(\Omega)$. Note that the nodes numbering is sequential (row by row, layer by layer), so the serial number of the node in position (i,j,k) is $i + (j-1) * n_x + (k-1) * n_x * n_y$.

The two-level Schwarz DD method is used as a preconditioner. On the first level, we suppose that Ω is decomposed into overlapping subdomains. The decomposition is only realized in the z direction, initially into nonoverlapping subdomains $\widehat{\Omega}_k$, which are subsequently extended to overlapping subdomains Ω_k,

$$\Omega = \bigcup_{k=1}^{p} \Omega_k. \tag{1.2}$$

The use of structural grids determines the overlapping as several layers of elements in z direction. The decomposition of Ω induces the decomposition of the space V,

$$V = V_1 + \ldots + V_p, \tag{1.3}$$

where

$$V_k = \{v \in V\colon\ v = 0 \text{ in } \Omega \setminus \Omega_k\}, \quad k = 1, \ldots, p. \tag{1.4}$$

Decomposition (1.3) allows to introduce both additive and multiplicative version of the DD preconditioner (see [12]). In our codes, we use the additive version of the overlapping Schwarz preconditioner, because the problems on the subdomains

are then independent, which makes the domain decomposition methods suitable for parallel computing. Note that the efficiency of the DD preconditioner improves with the increasing overlap. In the paper, we assume $2h$ size of the overlap (2 layers) for all numerical experiments, so the dependence of convergence on the size of the overlap is not tested.

The second level presents the extension of the FE space $V = V_h$ to the space $\overline{V}$ by adding the space V_0 for the coarse problem (see [13]),

$$\overline{V} = V_0 + V_1 + \ldots + V_p. \tag{1.5}$$

The use of the two-level preconditioner is very efficient in the case of an eliptic problem. The efficiency of the one-level preconditioners based on decomposition (1.3) decreases with increasing p, see e.g. [13]. The reduction of the global error depends on the frequency. High frequency components of the error are reduced rapidly, while low frequency components of the error are reduced only slowly. With increasing number of subspaces p, the subdomains Ω_i become smaller and the smooth part of the error, which cannot be reduced using the local solvers on the subdomains, grows. Hence, we need the coarse grid correction of smooth errors.

The other explanation of lower efficiency of the preconditioner based on the one-level additive DD is the following. For eliptic PDEs, the solution at any point depends on the right-hand side and the boundary conditions for the entire domain. However, the information about the right-hand side at one point is conveyed through to another point only by passing through all the intermediate subdomains, each of which muddles it up a bit more. Therefore, the solver must have some mechanism for the global communication of information at each iteration. It is realized by adding a coarse grid corrector.

One way how to define the coarse problem is to discretize the continuous problem on the coarse grid, so $V_0 = V_H$,

$$V_H(\Omega) = \{v \in C(\bar{\Omega}) \cap \mathcal{V}\colon\ v|_{e_H} \in P_1(e_H)\ \forall\, e_H \in \mathcal{T}_H(\Omega)\}. \tag{1.6}$$

Such coarse space is very efficient in the case of nested grids, where the coarse grid basis functions are obtained by a linear combination from the fine grid basis functions. The coarse grid space V_H ($H > h$) is then contained in the fine grid space V_h, $V_H \subset V_h$. Then V_H and V_h are fully compatible FE spaces and $V = \overline{V}$. This approach corresponds to a geometric multigrid (see [9]).

If the fine grid is very complicated, then a fully compatible coarse grid does not exist. These difficulties motivated the development of the Algebraic Multigrid (AMG) approach [7], which enables constructing the coarse problem matrix on the basis of information available from the fine grid matrix.

The aggregation techniques constitute one of possible approaches to algebraic multilevel methods. They originally appeared in the context of multigrid methods but they can be also applied in the multi-level Schwarz domain decomposition methods (see [14], [3]). The aggregation of unknowns can be easily defined by clustering of neighbouring nodes. If G is the set of all n_h nodes of the fine grid, then the clustering divides the set G into n_H disjoint subsets G_i, $i = 1, \ldots, n_H$ (aggregation of nodes), where $G = \bigcup G_i$, $i = 1, \ldots, n_H$, $G_i \cap G_j = \emptyset$, $i \neq j$. We call this type of aggregation the classical aggregation in this paper. Each of the subsets G_i, $i = 1, \ldots, n_H$, determines uniquely a ("fictitious") node of the coarse problem, n_H then presents the number of nodes of the coarse problem. We say "fictitious" node, because in fact the coarse grid may not exist explicitly.

To determine the aggregated stiffness matrix K^H of the order $m_H \times m_H$, where $m_H = 3 * n_H$ in 3D elasticity problem, it is necessary to define the corresponding $m_h \times m_H$ interpolation matrix $R^\top$ ($m_h = 3 * n_h$, where n_h is the number of nodes of the fine problem) and the restriction matrix R. Then we can write the relation

$$K^H = RK^hR^\top, \tag{1.7}$$

where K^h is the stiffness matrix for the fine grid problem. In the case of the classical aggregation, the restriction matrix R is the Boolen matrix with only one unity in each column. In this case, the coarse matrix row corresponding to a "fictitious" coarse grid node is given by the sum of the fine matrix rows corresponding to the nodes of the cluster of the neighbouring fine grid nodes. The aggregated basis functions are then defined as the sum of the fine grid basis functions for each cluster of unknowns (see [10]). The aggregated basis function has the value 1 in all clustered nodes and the value 0 in the remaining nodes.

The matrix created using this aggregation technique is too stiff. The difficulty is the high energy of these aggregated basis functions. This drawback can be avoided by smoothing the basis functions using the smoothed aggregations (see [15]), which are based on the smoothing of the partition of unity by smoothing a tentative interpolation vector. A newer approach smooths the partition of unity directly [8].

In the paper, we suggest a new smoothed aggregation technique (an overlapping aggregation technique), where the smoothing of the partition of unity is based on generalization of the aggregation for the fully compatible FE spaces. In the case of the fully compatible FE spaces, formulae for the relations between the coarse matrix elements and the fine matrix elements can be derived. In some problems, the fine grid is so complicated that the fully compatible coarse grid space does not exist. Those relations must be then modified.

We use structural grids with corresponding uniform rectangular "index" grids. If we define the coarse and fine grids FE spaces on these "index" grids, we obtain

in many cases fully compatible "index" FE spaces even for the original non fully compatible FE spaces. Consequently, we can modify the relations between the matrix elements derived for the fully compatible original FE spaces using index coordinates instead of real coordinates for the determinations of coefficients in the relations. In the case of noncompatible "index" grids, we use approximation of these coefficients.

The overlapping aggregation technique described in this paper differs from the "classical" AMG technique mentioned earlier. We have n_H groups G_i of nodes, $G = \bigcup G_i$, $i = 1, \ldots, n_H$, but the intersection of the neighbouring groups is not empty, $G_i \cap G_j \neq \emptyset$. The groups are overlapped. Each group determines a node for the coarse problem. It means that a fine grid node from the overlapping belongs to up to four groups G_i in the case of the FE coarse space based on tetrahedra and up to eight groups in the case of the FE coarse space based on hexahedra for structural grids. The restriction matrix R can then have 8 nonzero elements in each column. The column sums equal to 1.

If we write the matrix K^h in a block form, $K^h = (K^h_{ij})$, where K^h_{ij} are 3×3 blocks in 3D elasticity problem, then in the case of the classical aggregation technique, each block K^h_{ij} is added just to one corresponding block K^H_{ij} of the coarse problem matrix. In the overlapping aggregation technique, each block K^h_{ij} can be redistributed to several 3×3 blocks of coarse matrix rows which correspond to some neighbouring coarse grid nodes (up to 4 nodes in the case of the FE based on tetrahedra, up to 8 nodes for hexahedra). This redistribution is based on the relations between matrix blocks of stiffness matrices for the coarse and fine problems of nested grids (see next section). Note that the overlapping aggregation is very efficient in the case of strong heterogeneity. Unlike the classical aggregation, it redistributes the information from the fine grid node to all neighbouring coarse grid nodes.

The aggregation techniques were presented in many papers (see [7], [14], [15], [8]). In this paper, a different approach was used. The coarse grid matrix was assembled using a special ordering of fine grid nodes in the case of structural grids and by modification of relations between blocks of the fine and coarse grid matrices in the case of nested grids. The construction of the matrix for the coarse grid problem is the main and only result of the paper.

The paper is organized as follows. The construction of the coarse matrix for fully compatible grids using only the fine matrix elements is described in Section 2. Section 3 shows the process of determinating the aggregated matrix using the overlapping aggregations. In Section 4, the used solver for solving a system of linear algebraic equations is described. Finally, Section 5 presents the numerical results.

2. Construction of the matrix for a coarse grid

Assume that we have an FE model based on tetrahedral elements. Let Ω be a polytope domain and G_H be a coarse structural FE grid on Ω with corresponding nodes d_i^H, $i = 1, \ldots, n^H$. Let $\mathcal{T}_H(\Omega)$ be a corresponding set of tetrahedral elements. Note that Ω is firstly decomposed into hexahedral (generally nonrectangular) bricks, which are further decomposed, each brick into six tetrahedra. Similarly, let G_h be a fine structural FE grid on Ω with nodes d_i^h, $i = 1, \ldots, n^h$, and $\mathcal{T}_h(\Omega)$ be a corresponding set of tetrahedral elements. $V_H(\Omega)$, $V_h(\Omega)$ are the corresponding FE spaces (see (1.1), (1.6)).

We say that the divisions $\mathcal{T}_H$ and $\mathcal{T}_h$ are fully compatible if the elements $e_h \in \mathcal{T}_h$ arise from division of the elements $e_H \in \mathcal{T}_H$,

$$e_H = \bigcup e_h^k, \tag{2.1}$$

where e_h^k, $k = 1, \ldots, n_k^h$, are the tetrahedral elements from $\mathcal{T}_h$. In this case, any basis function N_i^H from the space V_H corresponding to the coarse grid node d_i^H can be written as

$$N_i^H = \sum_{k=1}^{n_i^h} \varphi_{ik} N_k^h, \tag{2.2}$$

where N_k^h, $k = 1, \ldots, n_i^h$, denote the standard basis functions of V_h corresponding to the fine grid nodes d_k^h, $k = 1, \ldots, n_i^h$, laying inside of the domain given by all coarse grid elements containing the coarse grid node d_i^H.

The relations $N_i^H(\mathbf{x}_j^H) = \delta_{ij}$, $N_i^h(\mathbf{x}_j^h) = \delta_{ij}$ hold, where $\mathbf{x}_j^H \in \mathbb{R}^3$ and $\mathbf{x}_j^h \in \mathbb{R}^3$ are the coordinates of the nodes d_j^H and d_j^h from G_H and G_h, respectively. Hence, we have the relation $\varphi_{ik} = N_i^H(\mathbf{x}_k^h)$ for any $i = 1, \ldots, n^H$, $k = 1, n_i^h$, which means that the value of the parameter φ_{ik} equals to the function value of N_i^H in the corresponding fine grid node d_k^h with the coordinate $\mathbf{x}_k^h$. If i, j, m, p are indices of the coarse grid nodes in the tetrahedron e_H, then the relation

$$N_i^H + N_j^H + N_m^H + N_p^H = 1 \tag{2.3}$$

holds on this tetrahedron. Then also the relation

$$\varphi_{ik} + \varphi_{jk} + \varphi_{mk} + \varphi_{pk} = 1 \tag{2.4}$$

holds in each node d_k^h from this tetrahedron. If the linear function $F(\mathbf{x})$ on the tetrahedron e_H with the node indices i, j, m, p has the nodal values $F(\mathbf{x}_i) = t_i$,

$F(\mathbf{x}_j) = t_j$, $F(\mathbf{x}_m) = t_m, F(\mathbf{x}_p) = t_p$, then we can express this function in a matrix form

$$F(\mathbf{x}) = [N_i^H(\mathbf{x}), N_j^H(\mathbf{x}), N_m^H(\mathbf{x}), N_p^H(\mathbf{x})]\mathbf{t}, \tag{2.5}$$

where $\mathbf{t} = (t_i, t_j, t_m, t_p)$. Note that in the case of the hexahedral FE, the relation (2.4) contains eight coefficients φ_{lk}.

In 3D elasticitity problems, the displacement of a point with the coordinates $\mathbf{x} = (x, y, z)$ is defined by three displacement components u, v, w in the direction of the three coordinates x, y, z,

$$\mathbf{u}(\mathbf{x}) = \left\{ \begin{array}{c} u(\mathbf{x}) \\ v(\mathbf{x}) \\ w(\mathbf{x}) \end{array} \right\}. \tag{2.6}$$

Using the FE method, we find the displacement $\mathbf{u}_h \in V_h(\Omega)^3$ (see [16]). We consider the same space of basis functions $V_h(\Omega)$ for each component. The following relations hold for both fine and coarse grids, so we omit parameters h and H. Here the index e marks an element both in the fine and coarse grids.

The displacement $\mathbf{u}_h$ in a tetrahedra element is determined by 12 displacement components of the corresponding four nodes as

$$\mathbf{a}^e = \left\{ \begin{array}{c} \mathbf{a}_i \\ \mathbf{a}_j \\ \mathbf{a}_m \\ \mathbf{a}_p \end{array} \right\} \tag{2.7}$$

with

$$\mathbf{a}_i = \left\{ \begin{array}{c} u_i \\ v_i \\ w_i \end{array} \right\} \text{ etc.}, \tag{2.8}$$

where u_i, v_i, w_i are the components of the displacement u, v, w in the node d_i. Similarly as in (2.5), we can write the displacement of arbitrary point in the element e as

$$\mathbf{u}(\mathbf{x}) = [\mathbf{I}N_i^e(\mathbf{x}), \mathbf{I}N_j^e(\mathbf{x}), \mathbf{I}N_m^e(\mathbf{x}), \mathbf{I}N_p^e(\mathbf{x})]\mathbf{a}^e, \tag{2.9}$$

where $\mathbf{I}$ is the 3×3 identity matrix and N_i^e, N_j^e, N_m^e, N_p^e are the basis functions corresponding to the nodes of the tetrahedral element e.

Using the known relations between displacements and deformations from the small deformation theory, the strain matrix on the element e can be defined as

$$\varepsilon = \begin{Bmatrix} \varepsilon_x \\ \varepsilon_y \\ \varepsilon_z \\ \gamma_{xy} \\ \gamma_{yz} \\ \gamma_{zx} \end{Bmatrix} = \begin{Bmatrix} \frac{\partial u}{\partial x} \\ \frac{\partial v}{\partial y} \\ \frac{\partial w}{\partial z} \\ \frac{\partial u}{\partial y} + \frac{\partial v}{\partial x} \\ \frac{\partial v}{\partial z} + \frac{\partial w}{\partial y} \\ \frac{\partial w}{\partial x} + \frac{\partial u}{\partial z} \end{Bmatrix}. \tag{2.10}$$

Using relation (2.9), the relation for the element e can be written as

$$\varepsilon = \mathbf{B}^e \mathbf{a}^e = [\mathbf{B}_i^e, \mathbf{B}_j^e, \mathbf{B}_m^e, \mathbf{B}_p^e]\mathbf{a}^e, \tag{2.11}$$

in which

$$\mathbf{B}_i^e = \begin{bmatrix} \frac{\partial N_i^e}{\partial x} & 0 & 0 \\ 0 & \frac{\partial N_i^e}{\partial y} & 0 \\ 0 & 0 & \frac{\partial N_i^e}{\partial z} \\ \frac{\partial N_i^e}{\partial y} & \frac{\partial N_i^e}{\partial x} & 0 \\ 0 & \frac{\partial N_i^e}{\partial z} & \frac{\partial N_i^e}{\partial y} \\ \frac{\partial N_i^e}{\partial z} & 0 & \frac{\partial N_i^e}{\partial x} \end{bmatrix} \tag{2.12}$$

with other submatrices obtained by interchanging subscripts. Note that the basis functions $N_i^e, N_j^e, N_m^e, N_p^e$ are linear on tetrahedral elements, so the partial derivatives exist inside the elements and are constant. If $\mathbf{D}^e$ is the 6×6 elasticity matrix containing appropriate material properties for the element e,

$$\mathbf{D}^e = \frac{E(1-\nu)}{(1+\nu)(1-2\nu)} \begin{bmatrix} 1 & \frac{\nu}{1-\nu} & \frac{\nu}{1-\nu} & 0 & 0 & 0 \\ \frac{\nu}{1-\nu} & 1 & \frac{\nu}{1-\nu} & 0 & 0 & 0 \\ \frac{\nu}{1-\nu} & \frac{\nu}{1-\nu} & 1 & 0 & 0 & 0 \\ 0 & 0 & 0 & \frac{1-2\nu}{2(1-\nu)} & 0 & 0 \\ 0 & 0 & 0 & 0 & \frac{1-2\nu}{2(1-\nu)} & 0 \\ 0 & 0 & 0 & 0 & 0 & \frac{1-2\nu}{2(1-\nu)} \end{bmatrix}, \tag{2.13}$$

where E is the Young's modulus, ν is the Poisson's ratio, then the element stiffness matrix is given by the relation (see [16])

$$\mathbf{K}^e = \int_e \mathbf{B}^{e\top} \mathbf{D}^e \mathbf{B}^e \, \mathrm{d(vol)}. \tag{2.14}$$

The matrices $\mathbf{B}^e$ and $\mathbf{D}^e$ are constant on the element e, so we can write relation (2.14) as

$$\mathbf{K}^e = \mathbf{B}^\top \mathbf{D}\mathbf{B} V^e, \tag{2.15}$$

where V^e is the volume of the element e. Note that in the case of the FE based on hexahedral elements, the basis funcions are trilinear and the matrices $\mathbf{B}^e$ and $\mathbf{D}^e$ are not constant. In this case, we can use the numerical integration to determine $\mathbf{K}^e$ in (2.14). If we use the decomposition

$$\mathbf{B}^e = [\mathbf{B}^e_i, \mathbf{B}^e_j, \mathbf{B}^e_m, \mathbf{B}^e_p], \tag{2.16}$$

then the local element matrix can be written in the block form

$$\mathbf{K}^e = \begin{bmatrix} \mathbf{K}^e_{ii} & \mathbf{K}^e_{ij} & \mathbf{K}^e_{im} & \mathbf{K}^e_{ip} \\ \mathbf{K}^e_{ji} & \mathbf{K}^e_{jj} & \mathbf{K}^e_{jm} & \mathbf{K}^e_{jp} \\ \mathbf{K}^e_{mi} & \mathbf{K}^e_{mj} & \mathbf{K}^e_{mm} & \mathbf{K}^e_{mp} \\ \mathbf{K}^e_{pi} & \mathbf{K}^e_{pj} & \mathbf{K}^e_{pm} & \mathbf{K}^e_{pp} \end{bmatrix}, \tag{2.17}$$

where the rs submatrix is the 3×3 matrix defined as

$$\mathbf{K}^e_{rs} = (\mathbf{B}^e_r)^\top \mathbf{D}^e \mathbf{B}^e_s V_e. \tag{2.18}$$

Here $r, s \in \{i, j, m, p\}$.

In the following part, we will distinguish between the coarse and fine grids using the corresponding indices H and h in the relations desribed above. We must note here that we assume homogeneous material on the subdomains corresponding to the individual coarse grid elements, so $\mathbf{D}^{e_h} = \mathbf{D}^{e_H}$ on this subdomain. Let e_H be the given coarse grid element and let $\{e^k_h\}$, $k = 1, \ldots, n_{e_H}$, be the corresponding set of fine grid elements, where $e_H = \bigcup\limits_k e^k_h$. We cannot use the expression for $N^{e_H}_i$ from (2.2) directly in (2.12) (and similarly for $N^{e_H}_j$, $N^{e_H}_m$, $N^{e_H}_p$), because the basis functions $N^{e_h}_i$ have not the partial derivatives on the fine grid element faces, but they exist inside the fine grid elements. Therefore, we rewrite relation (2.14) as

$$\mathbf{K}^{e_H} = \int_{e_H} (\mathbf{B}^{e_H})^\top \mathbf{D}^{e_H} \mathbf{B}^{e_H} \,\mathrm{d(vol)} = \sum_{e_h \subset e_H} \int_{e_h} (\mathbf{B}^{e_H})^\top \mathbf{D}^{e_H} \mathbf{B}^{e_H} \,\mathrm{d(vol)}. \tag{2.19}$$

Consequently, (2.18) has the form

$$\mathbf{K}^{e_H}_{rs} = \sum_{e_h \subset e_H} (\mathbf{B}^{e_H}_r)^\top \mathbf{D}^{e_H} \mathbf{B}^{e_H}_s V_{e_h} = \sum_{e_h \subset e_H} \mathbf{K}^{e_H}_{rs} | e_h. \tag{2.20}$$

Note that the notation $\mathbf{K}_{rs}^{e_H}|e_h$ denotes the contribution to the global coarse matrix from the local matrix for the fine grid element e_h. Because the derivatives of N_i^h, $i = 1, \ldots, n^h$, exist inside the element e_h, we can substitute N_i^H from (2.2) to (2.12), element by element.

Let the element e_h^k, $e_h^k \subset e_H$, have the nodes with the indices b, c, d, f and let the element e_H have the nodes with the indices i, j, m, p. Then relation (2.2) can be written as

$$N_r^{e_H}|e_h^k = \sum_{l \in \{b,c,d,f\}} \varphi_{rl} N_l^{e_h^k} \tag{2.21}$$

on e_h^k, $r \in \{i, j, m, p\}$. After substituting (2.21) to (2.12) and subsequently to (2.20), we can write the contribution from this element to the submatrix $\mathbf{K}_{rs}^{e_H}$ in (2.20) as

$$\mathbf{K}_{rs}^{e_H}|e_h^k = \sum_{g,l \in \{b,c,d,f\}} \varphi_{rg}\varphi_{sl}(\mathbf{B}_g^{e_h})^\top \mathbf{D}^{e_h} \mathbf{B}_l^{e_h} V_{e_h^k} = \sum_{g,l \in \{b,c,d,f\}} \varphi_{rg}\varphi_{sl}\mathbf{K}_{gl}^{e_h}, \tag{2.22}$$

where $V_{e_h^k}$ represents the volume of the element e_h^k. We can write similar relations for all submatrices $\mathbf{K}_{rs}^{e_H}|e_h^k$, $r, s \in \{i, j, m, p\}$. We can see from relations (2.22) that each block $\mathbf{K}_{rs}^{e_H}$ contains a weighted contribution from all blocks $\mathbf{K}_{gl}^{e_h}$ of the fine grid matrix corresponding to the connections between the nodes b, c, d, f. It means that for the FE based on tetrahedra, the matrix blocks are redistributed into up to 16 blocks of the coarse grid matrix. In the case of the hexahedral FE, these blocks can be redistributed even into up to 64 blocks with various weighted coefficients α_i, $\sum \alpha_i = 1$.

Relations (2.22) can be written in the matrix form as

$$\mathbf{K}^{e_H}|e_h^k = \mathbf{R}_{e_h^k} \mathbf{K}^{e_h^k} \mathbf{R}_{e_h^k}^\top, \tag{2.23}$$

where

$$\mathbf{R}_{e_h^k} = \begin{pmatrix} \varphi_{ib}\mathbf{I} & \varphi_{ic}\mathbf{I} & \varphi_{id}\mathbf{I} & \varphi_{if}\mathbf{I} \\ \varphi_{jb}\mathbf{I} & \varphi_{jc}\mathbf{I} & \varphi_{jd}\mathbf{I} & \varphi_{jf}\mathbf{I} \\ \varphi_{mb}\mathbf{I} & \varphi_{mc}\mathbf{I} & \varphi_{md}\mathbf{I} & \varphi_{mf}\mathbf{I} \\ \varphi_{pb}\mathbf{I} & \varphi_{pc}\mathbf{I} & \varphi_{pd}\mathbf{I} & \varphi_{pf}\mathbf{I} \end{pmatrix}. \tag{2.24}$$

Here $\mathbf{I}$ is the 3×3 identity matrix, $\varphi_{gl} = N_g^{e_H}(\mathbf{x}_l^h)$, $g \in \{i, j, m, p\}$, $l \in \{b, c, d, f\}$, and

$$\mathbf{K}^{e_h^k} = \begin{bmatrix} \mathbf{K}_{bb}^{e_h^k} & \mathbf{K}_{bc}^{e_h^k} & \mathbf{K}_{bd}^{e_h^k} & \mathbf{K}_{bf}^{e_h^k} \\ \mathbf{K}_{cb}^{e_h^k} & \mathbf{K}_{cc}^{e_h^k} & \mathbf{K}_{cd}^{e_h^k} & \mathbf{K}_{cf}^{e_h^k} \\ \mathbf{K}_{db}^{e_h^k} & \mathbf{K}_{dc}^{e_h^k} & \mathbf{K}_{dd}^{e_h^k} & \mathbf{K}_{df}^{e_h^k} \\ \mathbf{K}_{fb}^{e_h^k} & \mathbf{K}_{fc}^{e_h^k} & \mathbf{K}_{fd}^{e_h^k} & \mathbf{K}_{ff}^{e_h^k} \end{bmatrix} \tag{2.25}$$

is the local fine grid matrix on the element e_k^h. In the matrix $\mathbf{R}_{e_h^k}$ the sum of the elements in each column equals to 1 (see (2.4)). Finally,

$$\mathbf{K}^{e_H} = \sum\nolimits_{e_h \subset e_H} \mathbf{K}^{e_H} | e_h^k. \tag{2.26}$$

The matrix $\mathbf{K}^{e_H}$ is the 12×12 local element stiffness matrix. The indices of the matrix correspond to the global indices of the global stiffness matrix of the order $m_H \times m_H$, where $m_H = 3 * n_H$ is the global number of unknowns for the coarse problem. For the transformation of the blocks from the local matrix to the global matrix, we use a transformation matrix. Let $\mathbf{S}^{e_H}$ be the $m_H \times 12$ transformation matrix corresponding to the element e_H. Then we can write

$$\mathbf{K}_H = \sum_{e_H \in \mathcal{T}_H(\Omega)} \mathbf{S}^{e_H} \mathbf{K}_H^{e_H} \mathbf{S}^{e_H \top} = \sum_{e_H \in \mathcal{T}_H(\Omega)} \mathbf{S}^{e_H} \Bigg(\sum_{e_h \subset e_H} \mathbf{R}_{e_h^k} \mathbf{K}^{e_h^k} \mathbf{R}_{e_h^k}^{\top} \Bigg) \mathbf{S}^{e_H \top}. \tag{2.27}$$

Relation (2.27) gives the rule how the 3×3 blocks of the local matrices $K^{e_h^k}$ for the fine grid problem are redistributed to the 3×3 blocks of the global stiffness matrix for the coarse grid problem. Consequently, we can rewrite relation (2.27) as

$$\mathbf{K}^H = \mathbf{R} \mathbf{K}^h \mathbf{R}^{\top} \tag{2.28}$$

with the $m^H \times m^h$ restriction matrix $\mathbf{R}$, $m_H = 3 * n^H$, and $m_h = 3 * n^h$. The column sums of the matrix $\mathbf{R}$ are equal to 1. Note that for fully compatible divisions $\mathcal{T}_H$ and $\mathcal{T}_h$, relation (2.28) gives the aggregated matrix which is identical with the coarse grid matrix assembled from the local coarse grid matrices if the material is homogeneous on the subdomains corresponding to the individual coarse grid elements. Note that relation (2.28) can be used even when the condition of homogeneity is not fulfilled.

3. Construction of the overlapping aggregations

The construction of the coarse grid matrix described in Section 2 assumes that there exists an FE space $V_H(\Omega)$ such that the divisions $\mathcal{T}_H$ and $\mathcal{T}_h$ are fully compatible. But for a general nonrectangular structural grid, a fully compatible coarse FE space may not exist and relations (2.19)–(2.23) cannot be used. As we mentioned in Section 1, the general structural grid on Ω corresponds to the rectangular uniform "index" grid on the corresponding domain Ω^{index} (Ω^{index} is a rectangular polytope domain with dimension $\langle 1, n_x \rangle \times \langle 1, n_y \rangle \times \langle 1, n_z \rangle$). For this "index" grid we can define a set of elements $\mathcal{T}(\Omega^{\text{index}})$ and a corresponding FE space $V(\Omega^{\text{index}})$. Note that the "index" elements can be tetrahedra or hexahedra.

Let I_h be a fine "index" grid. We can construct the "index" coarse grid I_H in such a way that the nodes from I_H will be identical with some nodes from the "index" fine grid I_h. The condition to be fulfilled is that all nodes from the coarse grid index "line" (e.g. nodes $\{i_1, j_1, k\}$, $k = 1, n_z^H$) have to belong to the same fine grid index "line" (Figure 1(a)). Note that an "index" coarse grid determines the coarse grid G_H on the real coordinates x, y, z.

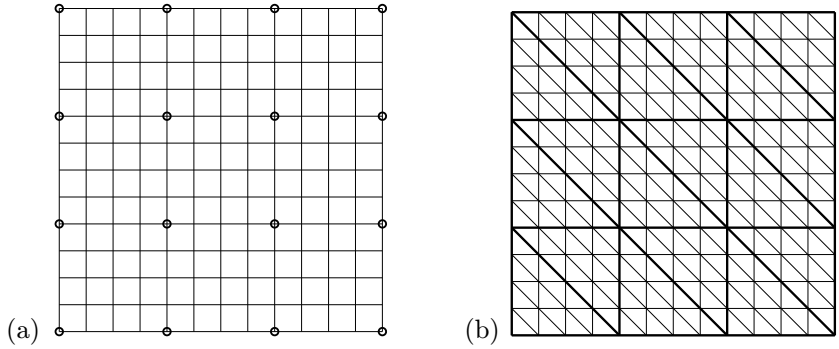

Figure 1. (a) Position of coarse grid nodes, (b) Triangularization-fully compatible grids.

Let n_x^H, n_y^H, n_z^H be the numbers of the coarse grid nodes in the corresponding directions. If we have the "index" grid I_h, then for the FE space $V_h(\Omega^{\text{index}})$ based on the hexahedral elements, the fully compatible FE space $V_H(\Omega^{\text{index}})$ always exists. Different situation occurs when the "index" FE space is based on tetrahedral elements. Here, some necessary conditions have to be fulfilled so that the fully compatible "index" FE spaces are obtained. First, every coarse grid hexahedron must be refined by the same number of fine grid nodes in each direction. We must consider it during preparation of a fine grid and choose corresponding numbers of the fine grid nodes in each direction. Second, every hexahedron of the fine grid is decomposed into six tetrahedral elements. There exist 72 various conform decompositions into tetrahedra (see [11]). The necessary condition for fully compatible FE spaces is the same decomposition of all fine grid hexahedra contained in the corresponding coarse grid hexahedron (see the cross-section in Figure 1(b)).

The idea of the overlapping aggregation technique is the following. If the divisions $\mathcal{T}_H(\Omega^{\text{index}})$ and $\mathcal{T}_h(\Omega^{\text{index}})$ are fully compatible, we can derive a similar relation between the "index" coarse and the "index" fine matrix blocks as in (2.22) with different matrix $\mathbf{B}^{e_h}$ and with different coefficients φ_{rg}. This new relation is based on the relation

$$N_r^{\text{index},H} = \sum_{l=1}^{n_l^h} \widetilde{\varphi}_{rl} N_l^{\text{index},h}, \tag{3.1}$$

where $N_r^{\text{index},H}$ and $N_l^{\text{index},h}$ are the basis functions of the spaces $V_H(\Omega^{\text{index}})$ and $V_h(\Omega^{\text{index}})$, respectively. In the overlapping aggregation technique, we use relations (2.22), but we replace the coefficients φ_{rl} by $\widetilde{\varphi}_{rl}$ from relation (3.1) for the "index" basis functions.

So using the index grid coordinates instead of the real coordinates for the determination of the coefficients $\widetilde{\varphi}$, we modify the relations from Section 2 in such a way that we replace the coefficients φ_{rs} by the coefficients $\widetilde{\varphi}_{rs}$ in all relations. Then we rewrite relation (2.28) for the stiffness matrix as

$$\mathbf{K}^H = \widetilde{\mathbf{R}}\mathbf{K}^h\widetilde{\mathbf{R}}^\top, \tag{3.2}$$

where the matrix elements of $\widetilde{\mathbf{R}}$ are given by the coefficients $\widetilde{\varphi}_{rl}$ instead of φ_{rl}. As an illustration, we can see the 1D basis functions for the classical aggregation and the overlapping aggregation in Figures 2(a) and 2(b). Note that these basis functions serve only for constructing the coarse grid matrix.

The coarse grid G_H is "fictitious" in a sense. Therefore, we have to assume some triangularization of this grid to construct the corresponding function space $V_H(\Omega)$. Then the solution of the coarse problem meets the requirements for being an error corrector.

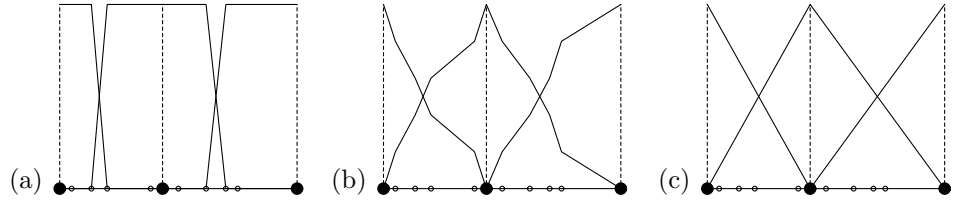

Figure 2. 1D basis function for (a) classical aggregation AG1, (b) overlapping aggregation AG2 based on "index" grid coefficients, (c) overlapping aggregation AG4 based on distances.

The determination of the matrix $\widetilde{\mathbf{R}}$ is based on relation (3.1). Relation (3.1) determines an important property of the matrix $\widetilde{\mathbf{R}}$—the column sums are equal to one.

We must note here that in the case of the structural grids, the stiffness matrix rows in 3D have maximum 81 nonzero elements, which corresponds to 27 nonzero blocks for each block row corresponding to one node.

Four types of aggregation techniques used in our codes are presented below.

(a) The "classical" aggregation technique (label AG1).

As we have already mentioned in the Introduction, in the "classical" aggregation technique the coarse grid matrix row corresponding to the coarse grid node is constructed as the sum of all fine grid matrix rows corresponding to the cluster of the neighbouring fine grid nodes. If we enumerate the nodes in the coarse grid and fine

grid elements locally in the same way, the coefficients $\widetilde{\varphi}_{ij}$ in (2.22) fulfill the relation $\widetilde{\varphi}_{ij} = \delta_{ij}$. It means that each block from the fine grid matrix is added to just one coarse grid matrix block and the matrix $\widetilde{\mathbf{R}}$ is the Boolean matrix with just one unity in each column. Other column elements are equal to zero. This type of aggregation is efficient in the case of homogeneous material on uniform grids.

(b) The overlapping aggregation based on tetrahedra (label AG2).

This type of aggregation is based on relation (3.1) for the fully compatible "index" FE spaces with tetrahedral elements. For the determination of coefficients we use the basis functions of the "index" coarse grid FE space $V_H(\Omega_{\text{index}})$. Then $\widetilde{\varphi}_{ij} = N_i^{\text{index},H}(\mathbf{x}_j^{\text{index}})$. As we have mentioned earlier there exist 72 various conformed decompositions of a hexahedron into 6 tetrahedra. To determine the coefficients $\widetilde{\varphi}_{ij}$, we must explicitly know the basis functions on individual tetrahedral elements for every decomposition. It is arduous to construct all these basis functions. Therefore, we suppose that all "index" coarse grid hexahedra are decomposed into tetrahedra in the same way (given in advance). This new decomposition generates new basis functions $N_r^{\text{index},H}$, $N_l^{\text{index},h}$, which we use in relation (3.1).

Basis functions for the decomposition presented in Figure 3(b) are the folowing. Let the unit cube be the "index" coarse grid hexahedron (Figure 3(a)). The nodes have then the index coordinates:

node $\mathbf{1} = (0,0,0)$, node $\mathbf{2} = (1,0,0)$, node $\mathbf{3} = (0,1,0)$, node $\mathbf{4} = (1,1,0)$,

node $\mathbf{5} = (0,0,1)$, node $\mathbf{6} = (1,0,1)$, node $\mathbf{7} = (0,1,1)$, node $\mathbf{8} = (1,1,1)$.

We suppose the "index" tetrahedron being decomposed into the following 6 tetrahedra: **1438**, **1837**, **1875**, **1568**, **1248**, **1268** (see Figure 3(b)).

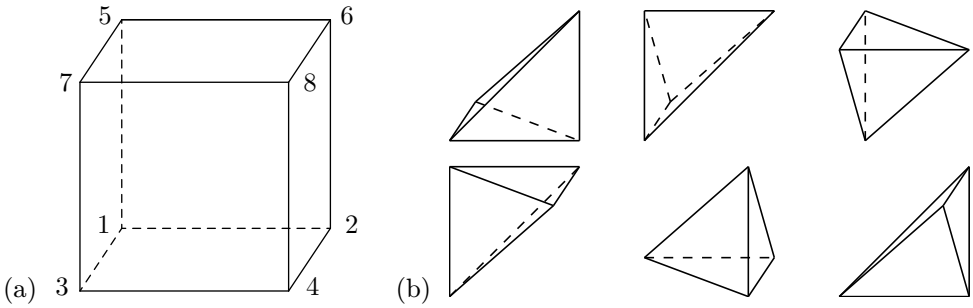

Figure 3. (a) Hexahedral "index" element, (b) Division into tetrahedra.

The basis functions for these tetrahedra are presented in Table 1.

Now we can simply determine the coefficients $\widetilde{\varphi}_{ij}$. E.g., if a fine grid node has the local index coordinates $\mathbf{x}_k = (\frac{2}{4}, \frac{3}{4}, \frac{1}{4})$, then this node is inside the tetrahedron **1438** and the corresponding coefficients have the values $\widetilde{\varphi}_{1k} = \frac{1}{4}$, $\widetilde{\varphi}_{3k} = \frac{1}{4}$, $\widetilde{\varphi}_{14} = \frac{1}{4}$, $\widetilde{\varphi}_{18} = \frac{1}{4}$.

1438:	$1-y$	$x-z$	$y-x$	z
1837:	$1-y$	x	$y-z$	$z-x$
1875:	$1-z$	x	$y-x$	$z-y$
1568:	$1-z$	$z-x$	$x-y$	y
1248:	$1-x$	$x-y$	$y-z$	z
1268:	$1-x$	$x-z$	$z-y$	y

Table 1. Basis functions for individual tetrahedra.

This type of aggregation requires fulfilment of an important condition. The numbers of the fine grid nodes in individual directions must enable constructing the coarse grid in such a way that every coarse hexahedron contains the same number of fine grid nodes in all three directions. Then the "index" FE spaces for this new decomposition are fully compatible. If this condition is not fulfilled, relation (3.1) is not valid. Nevertheless, we can use the relation $\widetilde{\varphi}_{ij} = N_i^{\mathrm{index},H}(\mathbf{x}_j^{\mathrm{index}})$ to determine the coefficients $\widetilde{\varphi}_{ij}$ even in this case .

In this type of aggregation, the matrix $\widetilde{\mathbf{R}}$ has at most four nonzero elements in each column and their sum is equal to one. Then each 3×3 fine matrix block is weight-redistributed into at most sixteen 3×3 coarse matrix blocks. The sum of the weight coefficients is equal to 1.

(c) The overlapping aggregation based on hexahedra (label AG3).

Despite the fact that the FE space $V_h(\Omega)$ can be based on tetrahedra, this type of aggregation is based on relation (3.1) for trilinear basis functions of the FE spaces $V_h(\Omega_{\mathrm{index}})$ and $V_H(\Omega_{\mathrm{index}})$ based on hexahedra. The advantage of this approach is that the "index" FE spaces $V_h(\Omega_{\mathrm{index}})$ and $V_H(\Omega_{\mathrm{index}})$ are always fully compatible and we are not dependent on the type of decomposition of a hexahedron into a tetrahedra. All "index" hexahedral elements are unit cubes (see Figure 3(a)). The basis functions corresponding to the individual nodes are presented in Table 2.

$N_1^{\mathrm{index},H} = (1-x)(1-y)(1-z)$
$N_2^{\mathrm{index},H} = x(1-y)(1-z)$
$N_3^{\mathrm{index},H} = (1-x)y(1-z)$
$N_4^{\mathrm{index},H} = xy(1-z)$
$N_5^{\mathrm{index},H} = (1-x)(1-y)z$
$N_6^{\mathrm{index},H} = x(1-y)z$
$N_7^{\mathrm{index},H} = (1-x)yz$
$N_8^{\mathrm{index},H} = xyz$

Table 2. Basis functions corresponding to the individual nodes in a hexahedron.

In this type of aggregation, the matrix $\widetilde{\mathbf{R}}$ has at most eight nonzero elements in each column and their sum is equal to one. Then each 3×3 fine matrix block is weight-redistributed into at most sixty four 3×3 coarse matrix blocks (see (2.22)). If we number the nodes in a hexahedron locally by numbers 1–8 (see Figure 3(a)), then each 3×3 matrix block corresponding to a fine grid node inside the hexahedron is contributed (with weight coefficient) to the coarse grid matrix blocks $\mathbf{K}_{rs}^{e_H}$, $r, s = 1, \ldots, 8$. The weight coefficients α_{ij}^{rs} are given by the relation

$$\alpha_{ij}^{rs} = \widetilde{\varphi}_{ri}\widetilde{\varphi}_{sj} = N_r^{\mathrm{index},H}(\mathbf{x}_i^{h,\mathrm{index}})N_s^{\mathrm{index},H}(\mathbf{x}_j^{h,\mathrm{index}}). \tag{3.3}$$

For instance, the contribution of the fine matrix block $\mathbf{a}_{ij}$ (the node i with local coordinates $\mathbf{x}_i = (\frac{1}{4}, \frac{3}{5}, \frac{1}{3})$, the node j with local coordinates $\mathbf{x}_j = (\frac{2}{4}, \frac{4}{5}, \frac{2}{3})$) to the coarse matrix block $\mathbf{K}_{12}$ has the weight coefficient which equals to the value

$$\alpha_{ij}^{12} = (1 - x_i)(1 - y_i)(1 - z_i)x_j(1 - y_j)(1 - z_j) = 0.00666.$$

(d) The overlapping aggregation based on distances between nodes (label AG4).

The aggregation AG2 and AG3 determine the coefficients $\widetilde{\varphi}_{ij}$ using nodal values of the "index" coarse grid basis functions $N_i^{\mathrm{index},H}$. Thus, the "index" coordinates do not respect the real distances between the nodes. These types of aggregations are very efficient for uniform grids, but they may not be efficient enough for strongly nonuniform grids. Therefore, we introduce another type of aggregation which is based on hexahedra, but the coefficients of which are not determined using the basis functions. To determine the coefficients, the real distances between the nodes are used.

Let u, v, w be the functions defined only for the fine grid nodes, other function values are irrelevant. If the coarse grid hexahedron contains $m_x \times m_y \times m_z$ fine grid nodes, then for the fine grid node with the local indices (i, j, k), the function values of the functions u, v, w in the node $\mathbf{x}_{ijk} = (x_{ijk}, y_{ijk}, z_{ijk})$ are the following (see Figure 4—a projection of index xz cross-section with $C = \mathbf{x}_{ijk}$, $A = \mathbf{x}_{ij1}$,

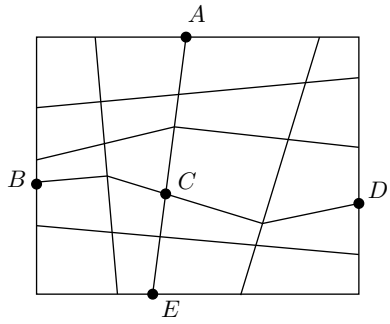

Figure 4. Grid for AG4.

$E = \mathbf{x}_{ijm_z}$, $B = \mathbf{x}_{1jk}$, $D = \mathbf{x}_{m_xjk}$, in addition $F = \mathbf{x}_{i1k}$ is a node on the index xy cross-section for $j = 1$ and $G = \mathbf{x}_{im_yk}$ is a node on the index xy cross-section for $j = m_y$):

$$u(C) = \frac{\operatorname{dist}(C,B)}{\operatorname{dist}(C,B) + \operatorname{dist}(C,D)}, \tag{3.4}$$

$$v(C) = \frac{\operatorname{dist}(C,F)}{\operatorname{dist}(C,F) + \operatorname{dist}(C,G)}, \tag{3.5}$$

$$w(C) = \frac{\operatorname{dist}(C,A)}{\operatorname{dist}(C,A) + \operatorname{dist}(C,B)}. \tag{3.6}$$

So the basis functions $N_i^{\text{index},H}$ (Table 2) are modified to the functions F_i based on the distances between the nodes (see Table 3). The 1D basis function is presented in Figure 2(c).

$F_1 = (1-u(x,y,z))(1-v(x,y,z))(1-w(x,y,z))$
$F_2 = u(x,y,z)(1-v(x,y,z))(1-w(x,y,z))$
$F_3 = (1-u(x,y,z))v(x,y,z)(1-w(x,y,z))$
$F_4 = u(x,y,z)v(x,y,z)(1-w(x,y,z))$
$F_5 = (1-u(x,y,z))(1-v(x,y,z))w(x,y,z)$
$F_6 = u(x,y,z)(1-v(x,y,z))w(x,y,z)$
$F_7 = (1-u(x,y,z))v(x,y,z)w(x,y,z)$
$F_8 = u(x,y,z)v(x,y,z)w(x,y,z)$

Table 3. Functions based on the distances between the nodes.

Results of numerical tests of these 4 types of aggregation are presented in Section 5.

4. Solution of linear systems

As we have mentioned in Introduction, for the solution of large linear systems $Au = f$ arising from the FE analysis of elasticity problems we use the preconditioned CG method, where the preconditioning is given by the additive overlapping two-level Schwarz method with the aggregated coarse matrix described in Section 3. The preconditioning represents an approximate solution of the equation

$$Bg^i = (B_1 + B_2)g^i = b - Au^i = r^i, \tag{4.1}$$

where B_1 is a part of the preconditioning for the first level, B_2 is a part of the preconditioning for the second level, r^i is the residual in the ith iteration of CG.

On the first level, the domain Ω is decomposed into overlapping subdomains only in the z direction and as preconditioning we use the domain decomposition methods with the additive Schwarz preconditioner,

$$B_1 = \sum R_i^\top A_i^{-1} R_i. \tag{4.2}$$

Here R_i represents the $m_h \times m_i^h$ restriction matrix, where m_i^h is the number of rows corresponding to nodes of the subdomain Ω_i (see (1.3)). To solve the subproblems, we must add boundary conditions on new boundaries of the subdomains. We assume normal zero displacements on these (inner) boundaries. Finite element discretization of linear elasticity problems leads to a system of linear equations with the stiffness matrix which has some positive off-diagonal entries. To use an incomplete factorization for the solution on subdomains, we need to replace matrices A_i by matrices C_i obtained after deleting the coupling between the unknowns which correspond to the nodal displacement in different coordinate directions,

$$B_1 = \sum R_i^\top C_i^{-1} R_i. \tag{4.3}$$

The matrices C_i can be modified to a diagonal form with diagonal blocks given by the displacement-decomposition approach (DiD-IF—see [2]). Then the incomplete factorization can be used.

On the second level, we solve the coarse problem using inner iterations,

$$B_2 = A_0^{-1}. \tag{4.4}$$

Here the matrix A_0 is the aggregated matrix assembled from the matrix A by the overlapping aggregation technique described in the previous section. The solution of the coarse problem is realized by the preconditioned CG with the preconditioning given by the displacement decomposition—the incomplete factorization technique (DiD-IF). Generally, the aggregated matrix can disturb some important matrix properties and the incomplete factorization is not stable. To overcome these problems, we use the lumping procedure on the diagonal displacement-decomposition blocks summing all positive offdiagonal elements in the row to the corresponding diagonal elements. Note that we also use the lumping procedure for the fine grid matrix if it is necessary.

The efficiency of the two-level Schwarz preconditioner depends on the inner relative accuracy ε_0 of the residuals (Euclidean norm) for solving the coarse grid problem, which can be relatively low. In this case, we lose the orthogonality of the searched directions in CG for the fine grid equations. This leads to the idea of improving the

algorithm by restoring the orthogonality with respect to the last m directions using the Gram-Schmidt process [5].

Solution of some practical problems of linear elasticity requires the use of the pure Neumann boundary conditions. The finite element discretization of this problem leads to the linear system $A_h u_h = b_h$ with the matrix A_h which is (theoretically) singular (see [5]). In this case, the null space $N(A_h)$ is not empty and is given by three independent rigid body translations w_h^1, w_h^2, w_h^3 and three independent rigid body rotations w_h^4, w_h^5, w_h^6. Due to a not ideal balance between volume and boundary forces and also due to roundoff errors, the system $A_h u_h = b_h$ can be slightly inconsistent. It means that we are interested in the generalization of the solution u_h by solving the equations

$$A_h u_h = b_h - P_N(b_h), \tag{4.5}$$

where $P_N(b_h)$ is the orthogonal projection to $N(A_h)$. The projection $P_N(b_h)$ can be constructed numerically,

$$P_N(b_h) = \sum \alpha_i w_h^i, \ \sum \alpha_i \langle w_h^i, w_h^j \rangle = \langle b_h, w_h^j \rangle \quad \text{for } j = 1, \ldots, 6. \tag{4.6}$$

The roundoff errors may cause instability, so we stabilize PCG by projecting all computed residuals back to the theoretical range $R(A_h)$.

If we simulate a laboratory uniaxial test, the constant normal displacements are given on two opposite sides of a cube and zero forces are given on other four sides. In this case, the null space $N(A_h)$ is given by two independet rigid body translations and one rigid body rotation. The coefficients α_i, $i = 1, \ldots, 3$, are computed similarly as in (4.6).

Note that the stopping criteria for both the fine and the coarse grid problems are given by relative accuracy ε of the residuals.

5. Numerical tests

For the solution of the linear systems the preconditioned CG method is used, where the preconditioning is given by the additive overlapping two-level Schwarz method with the aggregated coarse matrix described in Section 3. In our case, the domain is divided into m subdomains Ω_k only in z direction. The linear system is solved in parallel and the number of subproblems corresponds to the number of used processors.

The parallel computations were performed on Super Micro computer (symmetric multiprocessor) with 8× octa-core processor Intel Xeon E7-8837. The parallel programming used the OpenMP paradigm.

The efficiency of the suggested aggregation technique was tested on two model problems (see Figure 5). In both model problems, we used 24 cores. The orthogonality of searched directions was restored with respect to last 3 directions.

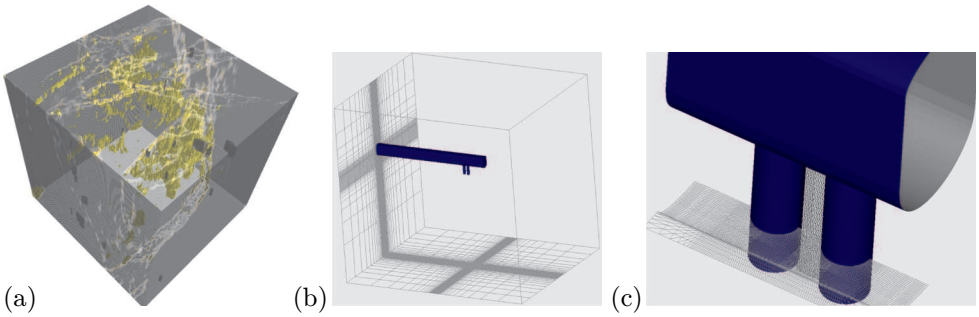

Figure 5. (a) Geocomposite model, (b) Äspö model—the global domain, (c) Detail of the grid.

(a) The first model (see Figure 5(a)) corresponds to the laboratory uniaxial test on a geocomposite (see [6]). The constant nonzero normal displacements are prescribed on the upper side of the cube, the zero normal displacements are prescribed on the bottom side of the cube. On the other sides we have prescribed zero normal forces. In this case, the null space is not empty and the projection of $R(A_h)$ described in the previous section has to be used. To test the efficience of the suggested aggregations, we used 5 different materials randomly distributed into the hexahedral elements. The distribution of materials was done algorithmically. In practice, the material distribution is determined using CT tomography. In our model problem, each material occupies 20 percents of the domain. We tested three different sets of material properties: homogeneous material (HOM), heterogeneous material (HET1) and strongly heterogeneous material (HET2) (see Table 4).

task/mat	mat1		mat2		mat3		mat4		mat5	
	E	ν	E	ν	E	ν	E	ν	E	ν
HOM	19000	0.20	19000	0.20	19000	0.20	19000	0.20	19000	0.20
HET1	19000	0.20	200000	0.30	5000	0.40	100000	0.25	1000	0.42
HET2	60000	0.20	600000	0.20	10000	0.40	200000	0.25	200	0.42

Table 4. Material properties for three different tasks.

These three material sets (HOM, HET1, HET2) were tested on three different rectangular grids: uniform (UN), nonuniform (NUN1) and strongly nonuniform (NUN2) (see Figure 6).

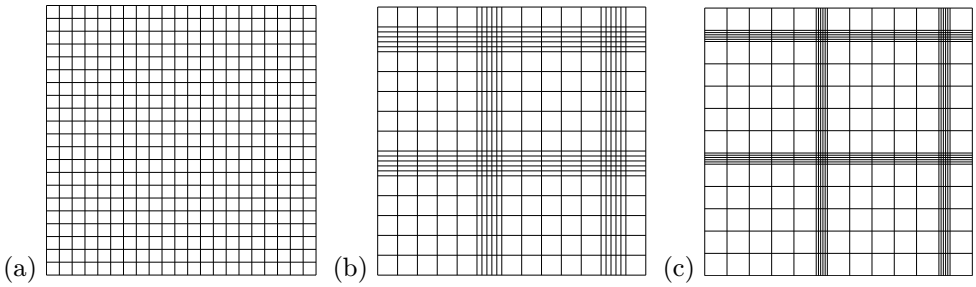

Figure 6. (a) Uniform grid (UN), (b) Nonuniform grid (NUN1), (c) Nonuniform grid (NUN2).

All three grids have dimensions of $401 \times 401 \times 401$ nodes (193 443 603 unknowns). The corresponding coarse grid has $41 \times 41 \times 41$ nodes (206 763 unknowns), so the grids are not fully compatible. The results of numerical tests are presented in Table 5. The numbers of outer iterations are in the upper part of the row, the numbers of inner iterations are in the lower part of the row. This table shows, that the overlapping aggregations are very efficient, especially in the case of strong nonuniformity of the grid.

	without aggreg	AG1	AG2	AG3	AG4
HOM	416	130	38	37	37
UN	–	2618	964	748	748
HOM	425	124	34	33	22
NUN1	–	2360	681	550	454
HOM	918	271	79	80	23
NUN2	–	4876	1342	1211	465
HET1	1030	259	68	69	69
UN	–	8262	2303	1839	1839
HET1	1314	412	87	87	77
NUN1	–	11013	2168	1755	2089
HET1	3723	1113	245	244	160
NUN2	–	33663	6720	5304	4046
HET2	1163	292	77	77	77
UN	–	9878	2639	2048	1839
HET2	1703	511	108	108	94
NUN1	–	14829	2560	2174	2549
HET2	4520	1328	274	269	184
NUN2	–	34723	5948	4954	4547
CPU time(s)	226877	79383	17936	16828	15782
CPU time/1 it	50.20	59.78	65.46	62.56	85.78

Table 5. Number of outer and inner iterations for various types of aggregation and the CPU time for the HET2-NUN2 task (geocomposite).

The iterations for the tasks with strongly anisotropic material (HET2) and with different nonuniformity of grids are presented in Figure 7. We can see that the aggregations AG2, AG3 and AG4 give similar convergence. Only in the case of the strong nonuniformity, the aggregation AG4 gives perceptibly better convergence. However, in all three cases, the convergence is significantly better than in the case of the classical aggregation AG1.

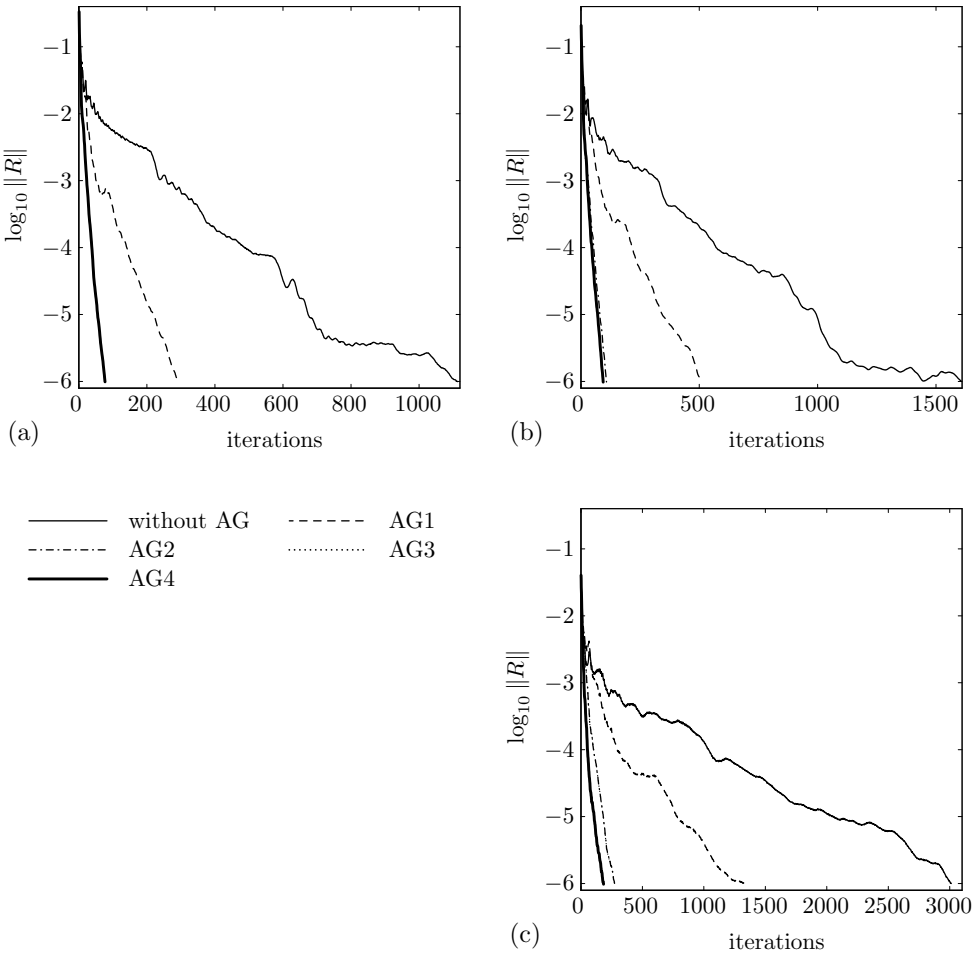

Figure 7. (a) HET2-UN task, (b) HET2-NUN1 task, (c) HET2-NUN2 task for geocomposite problem.

Similarly, we compared the graphs for the tasks with strong nonuniformity for different level of heterogeneity (see Figure 8). The results are similar to the results presented in Figure 7, but in this case the aggregation AG4 gives perceptibly better convergence in all three cases.

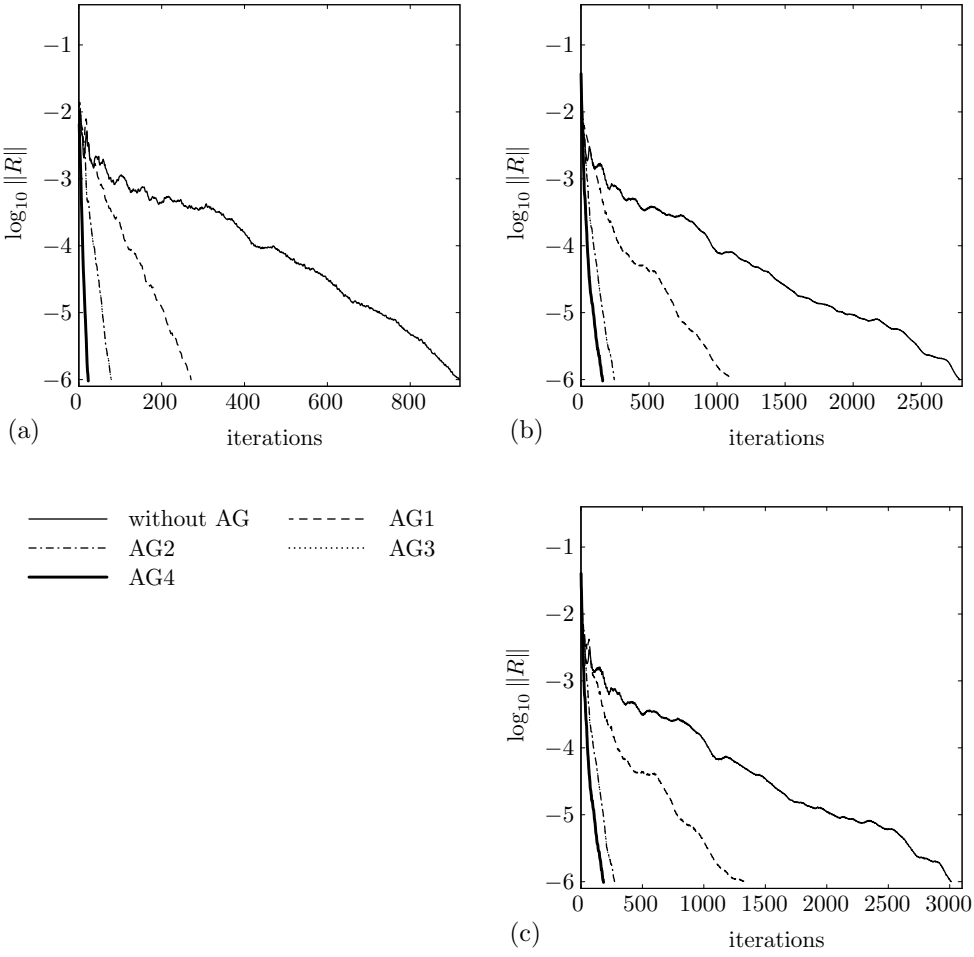

Figure 8. (a) HOM-NUN2 task, (b) HET1-NUN2 task, (c) HET2-NUN2 task for geocomposite problem.

(b) The second model problem comes from the Äspö Pillar Stability Experiment ([1]). The domain contains a long tunnel with two large holes (see Figure 5 (b)) in homogeneous rock ($E = 55\,000$ MPa, $\nu = 0.25$). The constant pressure is prescribed on the upper side of the domain, the normal zero displacements are prescribed on the other sides. The grid is more complicated (see Figure 5(c)) with the detail around the holes) and contains $295 \times 313 \times 291$ nodes (80 608 455 unknowns). We tested two coarse grids—$31 \times 31 \times 31$ nodes (89 373 unknowns) and $61 \times 61 \times 61$ nodes (680 943 unknowns). For the coarse grid $31 \times 31 \times 31$ we tested two variants—variant A with relative accuracy of the residuals for the inner iterations $\varepsilon = 0.001$, variant B with $\varepsilon = 0.1$. The results of numerical tests are presented in Table 6.

The number of outer iterations is in the upper part of the row, the number of inner iterations is in the lower part of the row.

coarse grid	without aggreg	AG1	AG2	AG3	AG4
$31 \times 31 \times 31$	3501	1260	1028	1028	962
variant A	–	67608	52364	191629	181573
$31 \times 31 \times 31$	3501	1287	1124	1066	984
variant B	–	5352	5671	23958	20186
$61 \times 61 \times 61$	3501	926	739	736	718
	–	67814	87954	246010	251942

Table 6. Number of outer and inner iterations for various types of aggregation (Äspö problem).

The corresponding graphs are presented in Figure 9.

The results show that the efficiency of the overlapping aggregation technique is not so good as in the case of rectangular grids in the geocomposite problem. Äspö model contains a long horizontal tunnel and two vertical holes. Using the structural grid for this problem generates elements that are not optimal. The stiffness matrix is ill-conditioned. The aggregated matrix is also ill-conditioned and the condition number depends on the type of aggregation (see Table 6—the numbers of inner iterations for AG2 and AG3).

6. Conclusion

We present the smoothed overlapping aggregation technique, where the smoothing is based on a generalization of the aggregation for fully compatible FE spaces formed on structural grids. The numerical tests show that the overlapping aggregations give good results in the case of rectangular grids, where both the original and the index grids are similar (and rectangular). This type of grids is typical in modelling of geocomposites, where the grids are prepared using computer tomography. For FE modelling of an area with tunnels, the use of structural grids gives very complicated grids and corresponding stiffness matrices are ill-conditioned. In this case, the index grid does not sufficiently correspond to the original grid. The grids are qualitatively quite different. The numerical tests show better results for the overlapping aggregations than for the classical aggregation technique. However, the improvement is not significant enough. The required improvement of convergence even under strong heterogeneity using the overlapping aggregation technique on structural grids is achieved if the grids are rectangular or close to rectangular.

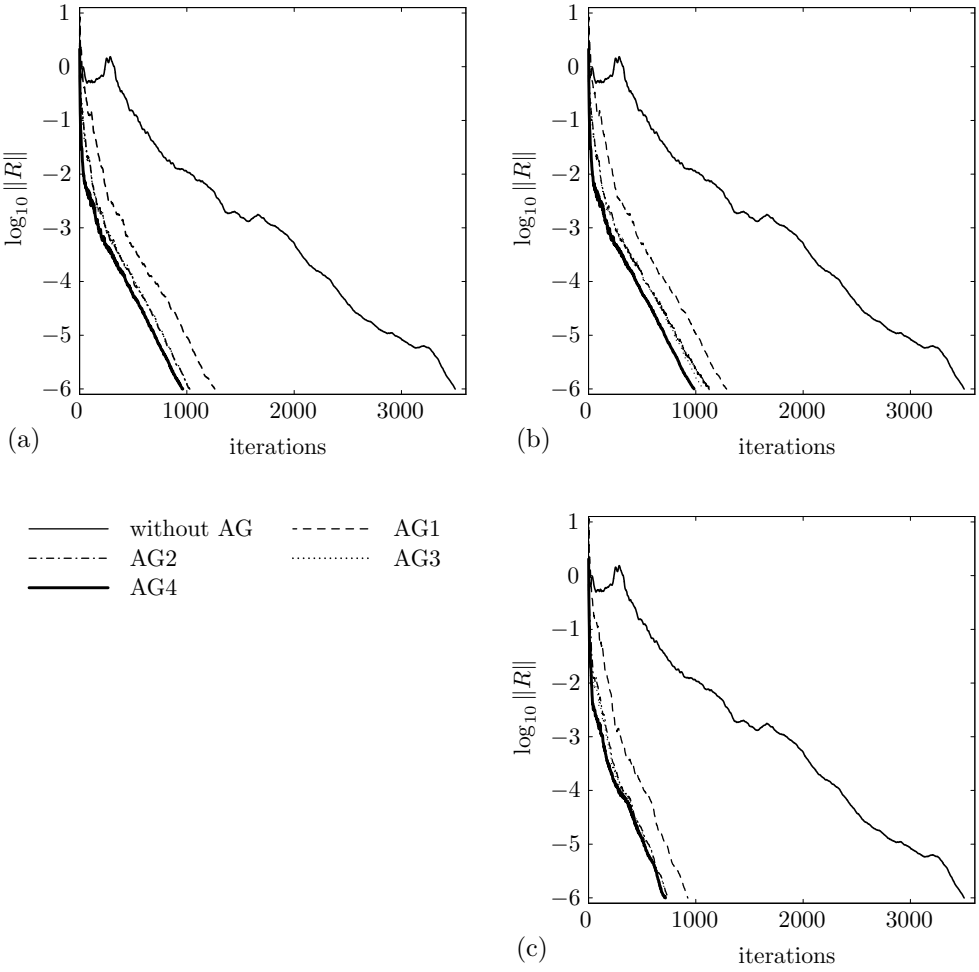

Figure 9. (a) Variant A with inner relative accuracy $\varepsilon = 0.001$, (b) Variant A with inner relative accuracy $\varepsilon = 0.1$, (c) Variant B with inner relative accuracy $\varepsilon = 0.001$ for the Äspö problem.

References

[1] *J. C. Andersson*: Rock Mass Response to Coupled Mechanical Thermal Loading: Äspö Pillar Stability Experiment. Doctoral Thesis. Byggvetenskap, Stockholm, 2007; Available at `http://urn.kb.se/resolve?urn=urn%3Anbn%3Ase%3Akth%3Adiva-4287`.

[2] *R. Blaheta*: Displacement decomposition—incomplete factorization preconditioning techniques for linear elasticity problems. Numer. Linear Algebra Appl. *1* (1994), 107–128. zbl MR doi

[3] *R. Blaheta*: Algebraic multilevel methods with aggregations: An overview. Large-Scale Scientific Computing (I. Lirkov et al., eds.). Lecture Notes in Computer Science 3743, Springer, Berlin, 2006, pp. 3–14. zbl MR doi

[4] *R. Blaheta, P. Byczanski, O. Jakl, J. Starý*: Space decomposition preconditioners and their application in geomechanics. Math. Comput. Simul. *61* (2003), 409–420. zbl MR doi
[5] *R. Blaheta, O. Jakl, R. Kohut, J. Starý*: Iterative displacement decomposition solvers for HPC in geomechanics. Large-Scale Scientific Computations of Engineering and Environmental Problems II (M. Griebel et al., eds.). Notes on Numerical Fluid Mechanics 73, Vieweg, Braunschweig, 2000, pp. 347–356. zbl
[6] *R. Blaheta, R. Kohut, A. Kolcun, K. Souček, L. Staš, L. Vavro*: Digital image based numerical micromechanics of geocomposites with application to chemical grouting. Int. J. Rock Mech. Min. Sci *77* (2015), 77–88. doi
[7] *A. Brandt, S. F. McCormick, J. W. Ruge*: Algebraic multigrid (AMG) for sparse matrix equations. Sparsity and Its Applications (D. J. Evans, ed.). Cambridge University Press, Cambridge, 1985, pp. 257–284. zbl MR
[8] *M. Brezina, T. Manteuffel, S. McCormick, J. Ruge, G. Sanders*: Towards adaptive smoothed aggregation (αSA) for nonsymmetric problems. SIAM J. Sci. Comput. *32* (2010), 14–39. zbl MR doi
[9] *W. Hackbusch*: Multi-grid Methods and Applications. Springer Series in Computational Mathematics 4, Springer, Berlin, 1985. zbl MR doi
[10] *E. W. Jenkins, C. E. Kees, C. T. Kelley, C. T. Miller*: An aggregation-based domain decomposition preconditioner for groundwater flow. SIAM J. Sci. Comput. *23* (2001), 430–441. zbl MR doi
[11] *A. Kolcun*: Conform decomposition of cube. SSCG'94: Spring School on Computer Graphics. Comenius University, Bratislava, 1994, pp. 185–191.
[12] *J. Mandel*: Hybrid domain decomposition with unstructured subdomains. Domain Decomposition Methods in Science and Engineering (A. Quarteroni et al., eds.). Contemporary Mathematics 157, American Mathematical Society, Providence, 1994, pp. 103–112. zbl MR doi
[13] *B. F. Smith, P. E. Bjørstad, W. D. Groop*: Domain Decomposition. Parallel Multilevel Methods for Elliptic Partial Differential Equations. Cambridge University Press, Cambridge, 1996. zbl MR
[14] *U. Trottenberg, C. W. Oosterle, A. Schüller*: Multigrid. Academic Press, New York, 2001. zbl MR
[15] *P. Vaněk, J. Mandel, M. Brezina*: Algebraic multigrid by smoothed aggregation for second and fourth order elliptic problems. Computing *56* (1996), 179–196. zbl MR doi
[16] *O. C. Zienkiewicz*: The Finite Element Method. McGraw-Hill, London, 1977. zbl

Author's address: *Roman Kohut*, Institute of Geonics, Academy of Sciences of the Czech Republic, Studentská 17, 708 00 Ostrava, Czech Republic, e-mail: `roman.kohut@ugn.cas.cz`.